Reprinted from the preprint volume of the **Fifth Conference on Polar Meteorology and Oceanography**, 10–15 January 1999, Dallas, TX, by the AMS, Boston, MA.

13.4

ASSIMILATION OF OBSERVED ICE MOTIONS INTO A SEA ICE THICKNESS DISTRIBUTION MODEL

Walter N. Meier*
University of Colorado, Boulder, Colorado

James A. Maslanik
University of Colorado, Boulder, Colorado

1. INTRODUCTION

Three primary approaches have traditionally been employed to gather information about the Arctic sea ice: in situ measurements, remote sensing, and modeling. Each of these basic approaches is valuable in its own right and provides useful information to increase understanding of sea ice processes. However, each method is limited in scope and is best suited to different tasks; none of the methods can completely characterize the sea-ice environment independently. By combining the myriad of parameters available from in situ measurements, satellites, and models in a coherent manner, it is possible to produce more complete and more accurate data sets. Data assimilation is one technique suited to such combination of disparate data types with modeling.

Assimilating data into numerical models has proven useful in the atmospheric modeling community for many years (e.g. Ghil and Malanotte-Rizzoli, 1991), and more recently in ocean (e.g. Kantha, 1995) and sea ice models (e.g. Thomas and Rothrock, 1993). Data assimilation has the potential to be mutually beneficial to both remote sensing and modeling of the Arctic.

A variety of remotely-sensed products are available that potentially lend themselves to assimilation applications within sea ice modeling. Here, we focus on newly-developed ice motion products available from passive microwave imagery acquired by the Special Sensor Microwave/Imager (SSM/I). The objective of this work is to (1) compare a year-long set of SSM/I-derived ice motions from 1992 with motions estimated using a two-dimensional sea ice thickness distribution model, and (2) investigate the effects of an optimal interpolation assimilation method on ice motion and other model fields.

2. OBSERVED AND MODELED ICE MOTIONS

2.1 *SSM/I Motions*

Ice motions have been successfully tracked using visible and infrared Advanced Very High Resolution Radiometer (AVHRR) (Ninnis, 1986; Emery et al., 1991) and synthetic aperture radar (SAR) ERS-1 (Kwok et al., 1990; 1995) sensors. However, these measurements are limited by areal coverage, time sampling, or clouds. Recent work has demonstrated the potential of passive microwave data for overcoming some of these limitations in spatial and temporal coverage (Agnew et al., 1997; Emery et al., 1997; Liu and Zhao, 1998; and Kwok et al., 1998).

The data set used here was derived from daily composite grids of brightness temperatures obtained from the National Snow and Ice Data Center (NSIDC) and a two-dimensional cross-correlation technique was used to match feature locations between image pairs (Emery et al., 1991; Emery et al., 1997). With a 12.5-kilometer resolution for the 85 GHz data, the nominal velocity resolution for daily motions is about 7.2 cm/s; oversampling of the data can improve the resolution by a factor of two. Retrieval of SSM/I motions during summer is limited by the presence of cloud cover and, probably, by the effects of surface melt. Comparisons discussed here are therefore restricted to autumn, winter, and spring months. Daily files of u and v components of velocity on the Pathfinder grid were then rotated to the model grid for comparison and assimilation with the model.

Holt et al. (1992) describe two primary error sources in measuring ice motion for remotely-sensed images: geolocation errors of image pixels and tracking errors from the cross-correlation technique. Assuming the errors to be uncorrelated and Gaussian with zero mean yields a theorectical total daily velocity error of 19.4 cm/s. In actuality, the geolocation error between images is often correlated to some extent and the total error approaches the tracking error. The tracking error is reduced via oversampling of the data and filtering of motions. Because the SSM/I motions are derived from daily composite images, an additional binning error results due to temporal and spatial smearing of the signal (Kwok et al., 1998).

2.2 *Model Motions*

Ice motions were estimated by a dynamic-thermodynamic basin model with a viscous-plastic rheology (Arbetter et al., 1998). It allows for the use of either a 2-category (open water/thin ice and thick ice) ice thickness distribution (ITD) based on Hibler (1979) or a 28 category ITD based on formulations by Thorndike et al. (1975) and Flato and Hibler (1995). Thermodynamics are from Hibler (1980). The inclusion of an ice thickness distribution in a sea ice model is beneficial because it prescribes thin ice categories where net heat input into the atmosphere can be considerably higher than over thicker ice. Daily National

* *Corresponding author address:* Walter N. Meier, Univ. of Colorado, Dept. of Aerospace Eng., Boulder, CO 80309-0431; email: walter.meier@colorado.edu

Center for Environmental Prediction (NCEP) Reanalysis (Kalnay et al., 1996) fields are used for atmospheric forcings. Motions are output as u and v components that are oriented with the SSM/I and buoy motions to a common grid.

2.3 *Buoy Motions*

Daily ice motions were also derived from International Arctic Buoy Program (IABP) buoy data. Buoy positions are accurate to within 350 m (Thorndike and Colony, 1980), which corresponds to a daily motion accuracy of about 0.7 cm/s. Buoy measurements are sparse (15 to 30 per day) and are not distributed uniformly, but because of their accuracy, they are useful in evaluating the quality of the SSM/I model motions. Buoy motions were compared to motions of the nearest model grid point for evaluation of error statistics.

3. ASSIMILATION OF SSM/I MOTIONS

Optimal interpolation is a statistical assimilation method that uses the error statistics of observations and model predictions to obtain a statistically optimal combination of the model value and available observations that minimizes error. The basic formulation is as follows:

$$u_k^{\text{assim}} = u_k^{\text{model}} + \sum_{i=1}^{N} a_{ki}\left(u_i^{\text{obs}} - u_i^{\text{model}}\right) \qquad (1)$$

where k is the model grid point and N is the total number of i observations assimilated at that grid point. The assimilation weights, a, are used to add an optimal linear combination of observed minus model residuals to the original model value and obtain a new assimilated value. The weights are determined based upon the relative accuracy of the observed and model values and the number and distribution of observations (Lorenc, 1981). The u and v components were assimilated independently. For clarity, stand-alone model runs without assimilation are referred to as 'model' cases and assimilated model runs with SSM/I motions are referred to as 'assimilation' cases.

The accuracy of the SSM/I and model motions and the effectiveness of the assimilation strategy was assessed through comparisons with 5328 co-located buoy observations during winter, spring and autumn of 1992. While less biased than the model motions, the SSM/I motions contain substantial noise due to the limits of the velocity resolution, resulting in higher error standard deviations and lower correlation with buoys (Table 1). The SSM/I statistics are comparable with other analyses (Kwok et al., 1998; Agnew et al., 1997).

Relative to buoy observations, assimilation substantially reduces the mean error of the model motions and the error standard deviations of both the model and SSM/I motions. Assimilation also increases the correlation with buoys over both the SSM/I and model motions. The assimilation process smoothes noise in the SSM/I motions and reduces bias in the model motions.

	u (cm/s)			v (cm/s)		
	ε	σ	ρ	ε	σ	ρ
SSM/I	0.16	5.85	0.55	-0.40	5.94	0.58
2-category ITD						
model	0.74	4.82	0.71	-0.62	5.26	0.71
assim	0.20	3.34	0.83	-0.41	3.42	0.84
28-category ITD						
model	0.79	4.69	0.71	-0.30	5.12	0.70
assim	0.29	3.31	0.84	-0.35	3.40	0.84

Table 1. Mean error, ε, error standard deviation, σ, and correlation with buoys, ρ, for SSM/I, stand-alone model and assimilation cases for both the 2-category ITD and the 28-category ITD.

The error reduction of the 28-category ITD model run over the 2-category ITD model run is small, particularly relative to the reduction by assimilation. This indicates that a suitable assimilation strategy may ameliorate errors in model estimates of ice motion more effectively than by increasing model complexity. Assimilation increases the computation time of the 2-category run by approximately 30%; the 28-category model run requires about twice as much time as the 2-category run. Thus, assimilation is also more efficient in terms of computation time.

4. ASSIMILATED MODEL ICE PRODUCTS

Since assimilation reduces errors in ice motion estimates, overall circulation patterns and other physical parameters that are influenced by ice motion should also be affected. To illustrate this, ice motion and ice thickness fields of the annual average difference between assimilation and model cases are examined (Figure 1). Relative to model motions, assimilation increases transport out of the Beaufort Sea, across the pole and through the Fram Strait and produces more convergent motion along the east Greenland coast. These patterns are apparent in both the 2-category and 28-category cases. Advection out of the Beaufort Sea is slightly more pronounced with the 2-category ITD, while advection towards the north Greenland coast is slightly larger in with the 28-category ITD.

These differences in ice motion also affect the mean ice thickness fields. In the 2-category case, assimilation produces up to 10 cm thinner ice in the Beaufort Sea and Central Arctic because of increased ice advection away from these areas (Figure 1c). Up to 15 cm thicker ice occurs along the east Greenland coast due to the increased convergent motion. However, even though the error statistics and mean motion perturbation patterns of the two ITD cases are similar, the 28-category assimilation case results in large changes in the average ice thickness near the Greenland coast and Canadian Archipelago (not shown). These changes are not physically realistic, which indicates that the 28-category ITD model may be overly sensitive to perturbations in advection caused by

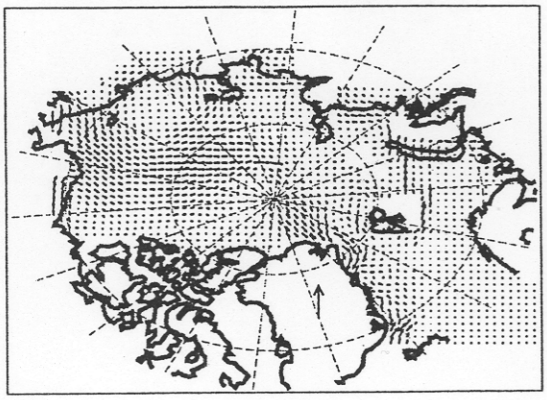

(a)

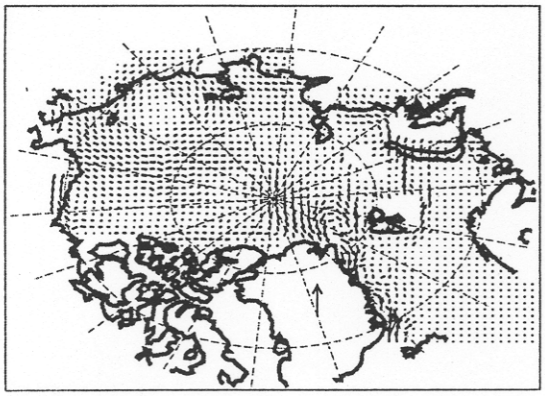

(b)

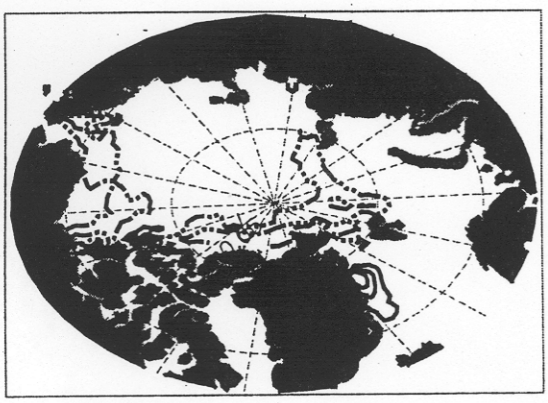

(c)

Figure 1. Annual average difference between assimilated fields and model fields: (a) assimilated – 2-cat. model motion; (b) assimilated – 28 cat. model motion; scale vector in both figures is 10 cm/s; (c) assimilated – 2-cat. model ice thickness, contours are 0.05 m. (solid contours are positive differences; dashed contours are negative differences).

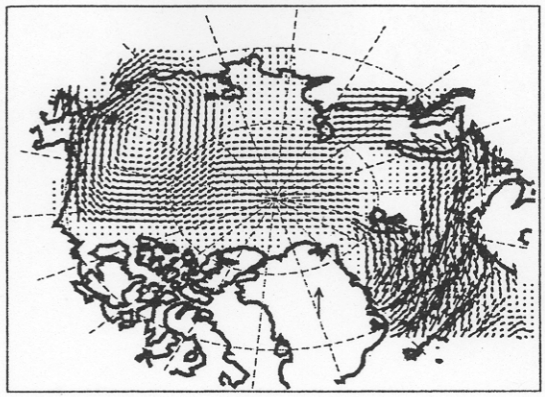

(a)

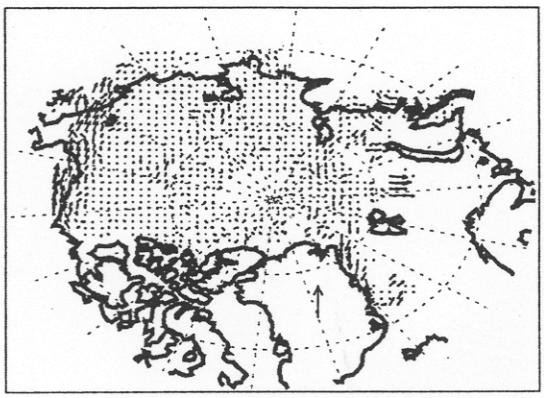

(b)

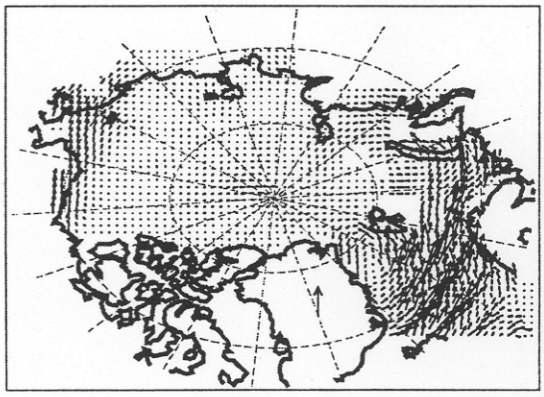

(c)

Figure 2. Ice motion fields on January 19, 1992: (a) model motion; (b) SSM/I motion; (c) assimilated motion. Scale vector in all three figures is 50 cm/s. Large motions in the Norwegian and Barents Seas for model and assimilation cases result from very low ice concentrations.

the observations. Modifying model parameters or reducing the assimilation weights may correct these advection overestimates. Nonetheless, this warrants further study.

5. JANUARY 1992 CASE STUDY

In addition to altering mean annual fields, assimilation can also substantially influence synoptic scale circulation. To demonstrate this, an example case-study motion field on January 19, 1992 is presented. On this day, high pressure is located over the Beaufort Sea. This is reflected in the model motions, which show the typical clockwise ice motion of the Beaufort Gyre (Figure 2a). However, the SSM/I field shows very little motion in this region, except adjacent to the Alaskan coast (Figure 2b). Comparison with buoy motions confirms that the SSM/I motions are correct and the model is overestimating velocities in this region. Thus, even though the model shows a reasonable circulation pattern for the given atmospheric conditions, this pattern is incorrect. This may be due to incorrect atmospheric forcings, or the ice interaction may be improperly parameterized for the given situation. Assimilation allows the SSM/I motions to correct the errors in the model motions, yielding a more accurate velocity field (Figure 2c).

6. CONCLUSION

This paper demonstrates the usefulness of applying assimilation techniques to improve ice motion estimates in the Arctic. The observations reduce model biases and constrain model motion to a realistic physical state. In turn, the model smoothes noise in the observations and fills in gaps where observations are absent or unreliable. Assimilation has potential to produce new observation-influenced fields, such as ice thickness, that are otherwise unavailable from remote sensing.

Assimilation of more accurate observations, such as from AVHRR or SAR, will improve ice motion estimates. Assimilation shows promise for Arctic applications beyond ice motion, such as albedo and ice temperature, although the implementation may not be as straightforward and suitable data sets may not be available. Other assimilation techniques, such as Kalman Filter or variational methods, may yield useful insights as well.

7. REFERENCES

Agnew, T., H. Le, and T. Hirose, 1997: Estimation of large scale sea ice motion from SSM/I 85.5 GHz imagery, *Ann. Glaciol.*, **25**, 305-311.

Arbetter, T.A., J.A. Curry, and J.A. Maslanik, 1998: Effects of rheology and ice thickness distribution in a dynamic-thermodynamic sea ice model, submitted to *J. Phys. Oceanogr.*

Emery, W.J., C.W. Fowler, J. Hawkins, and R.H. Preller, 1991: Fram Strait satellite image derived ice motions, *J. Geophys. Res.*, **96(C3)**, 4751-4768.

Emery, W.J., C.W. Fowler, J.A. Maslanik, 1997: Satellite-derived maps of Arctic and Antarctic sea ice motions: 1988-1994, *Geophys. Res. Letters*, **24**, 897-900.

Flato, G.M., and W.D. Hibler, III, 1995: Ridging and strength in modeling the thickness distribution of sea ice, *J. Geophys. Res.*, **100**, 18611-18626.

Ghil, M., and P. Malanotte-Rizzoli, 1991: Data assimilation in meteorology and oceanography, *Adv. in Geophysics*, **33**, 141-266.

Hibler, W.D., III, 1979: A dynamic thermodynamic sea ice model, *J. Phys. Oceanogr.*, **9**, 815-846.

Hibler, W.D., III, 1980: Modeling a variable thickness sea ice cover, *Mon. Weather Rev.*, **108**, 1943-1973.

Holt, B., D.A. Rothrock, and R. Kwok, 1992: Determination of sea ice motion from satellite images, in Microwave Remote Sensing of Sea Ice, edited by F.D. Carsey, AGU Geophysical Monograph 68, pp. 344-354.

Kalnay, E. and coauthors, 1996: The NCEP/NCAR 40-Year Reanalysis Project, *Bull. Amer. Meteor. Soc.*, **77**, 437-471.

Kantha, L.H., 1995: Barotropic tides in the global oceans from a nonlinear tidal model assimilating altimetric tides, 1. Model description and results, *J. Geophys. Res.*, **100(C12)**, 25283-25308.

Kwok, R., J.C. Curlander, R. McConnell, and S.S. Pang, 1990: An ice-motion tracking system at the Alaska SAR Facility, *IEEE J. Oceanic Eng.*, **15**, 1-44.

Kwok, R., D.A. Rothrock, H.L. Stern, and G.F. Cunningham, 1995: Determination of the age distribution of sea ice from Lagrangian observations of ice motion, *IEEE Trans. Geosci. And Rem. Sens.*, **33(2)**, 392-400.

Kwok, R., A. Schweiger, D.A. Rothrock, S. Pang, and C. Kottmeier, 1998: Sea ice motion from satellite passive microwave imagery assessed with ERS SAR and buoy motions, *J. Geophys. Res.*, **103(C4)**, 8191-8214.

Liu, A.K., and Y. Zhao, 1998: Sea ice motion from wavelet analysis of satellite data, *Proc. Eighth (1998) International Offshore and Polar Engineering Conference*, Montreal, May 24-29, 1998, 30-35.

Lorenc, A.C., 1981: A global three-dimensional multivariate statistical interpolation scheme, *Mon. Weather Rev.*, **109**, 701-721.

Ninnis, R.M., W.J. Emery, and M.J. Collins, 1986: Automated extraction of pack ice motion from advanced very high resolution radiometer imagery, *J. Geophys. Res.*, **91(C9)**, 10725-10734.

Thomas, D.R., and D.A. Rothrock, 1993: The Arctic Ocean ice balance: A Kalman smoother estimate, *J. Geophys. Res.*, **98(C6)**, 10053-10067.

Thorndike, A.S., D.A. Rothrock, G.A. Maykut, and R. Colony, 1975: The thickness distribution of sea ice, *J. Geophys. Res.*, **80**, 4501-4513.

Thorndike, A.S., and R. Colony, 1980: Arctic Ocean Buoy Program data report, 19 January 1979 – 31 December 1979, Polar Science Center, Univ. of Washington, Seattle.